Jurnal Pendidikan Kimia (JPKIM)
p-ISSN: 2085-3653| e-ISSN: 2549-3116
https://jurnal.unimed.ac.id/2012/index.php/jpk/index

OPEN ACCESS
10.24114/jpkim.v16i3.65195
J. Pendidik. Kim 2024, 16(3), 293 – 301

Original Research Article

Oxidized cellulose 2,2,6,6-tetramethylpiperidine-1-oxyl (TEMPO) for Mn(II) adsorption

I Putu Mahendra - *https://orcid.org/0000-0002-0805-4498*
Department of Chemistry, Faculty of Science, Institut Teknologi Sumatera, Lampung Selatan 35365, Indonesia

Venti Finaritan
Department of Chemistry, Faculty of Science, Institut Teknologi Sumatera, Lampung Selatan 35365, Indonesia

Dwi Liza Ramadiani
Department of Chemistry, Faculty of Science, Institut Teknologi Sumatera, Lampung Selatan 35365, Indonesia

Hiskia Harianja
Department of Pharmacy, Faculty of Pharmacy and Health Sciences, Unversitas Sari Mutiara Indonesia, Medan 20123, Indonesia

Khatarina Meldawati Pasaribu - *https://orcid.org/0000-0003-3411-6864*
Research Center for Biomass and Bioproducts, National Research and Innovation Agency of Indonesia (BRIN), Cibinong 16911, Indonesia

Corresponding authors: I Putu Mahendra (e-Mail: i.mahendra@ki.itera.ac.id)

Citation: Mahendra, I.P., Finaritan, V., Ramadiani, D.L., Harianja, H., & Pasaribu, K.M. (2024). Oxidized cellulose 2,2,6,6-tetramethylpiperidine-1-oxyl (TEMPO) for Mn(II) adsorption. Jurnal Pendidikan Kimia (JPKIM), 16(3), 3293 – 301. https://doi.org/10.24114/jpkim.v16i3.65195

ARTICLE INFO

Keywords:
Adsorption;
Cellulose;
Mn^{2+} metal waste;
TEMPO/NaOCl/NaBr modified cellulose;
Water

History:
- Received - 14 Nov 2024
- Revised - 28 Dec 2024
- Accepted - 28 Dec 2024

ABSTRACT

The presence of excess Mn^{2+} in water can result in unpleasant odors and tastes, and its consumption can lead to neurological disorders in humans. Adsorption using oxidized cellulose is an efficient method for removing Mn^{2+} ions. In this study, cellulose was oxidized using the TEMPO/NaOCl/NaBr system with varying NaOCl concentrations (5, 15, and 30 mmol/g) to identify the optimum conditions for Mn^{2+} adsorption. The carboxyl group content in the oxidized cellulose samples was 0.2393, 0.2435, and 0.2664 mmol/g, respectively. The adsorption efficiencies were 92.40%, 91.71%, and 91.43%, with the highest efficiency observed at 5 mmol/g NaOCl. The decrease in adsorption efficiency at higher NaOCl concentrations was attributed to the oxidation of secondary hydroxyl groups, forming undesirable ketone groups and disrupting the reaction pathway. FTIR analysis confirmed successful oxidation with a new absorption band at 1646 cm^{-1}. XRD analysis showed an increase in the crystalline index to 82.8%, 83.1%, and 83.13% for NaOCl concentrations of 5, 15, and 30 mmol/g, respectively. This study highlights the potential of TEMPO/NaOCl/NaBr-oxidized cellulose as an effective adsorbent for Mn^{2+} removal under optimized conditions.

Introduction

Water is an essential resource for all living organisms, including plants, animals, and humans, as it is crucial for drinking and other daily needs (Sawka et al., 2005). However, water sources such as rivers are often contaminated by improper disposal of household, agricultural, and industrial waste (Zamora-Ledezma et al., 2021). Polluted water frequently contains heavy metals like Zn^{2+}, Cr^{6+}, Fe^{2+}, Mn^{2+}, Cu^{2+}, Pb^{2+}, and Al^{3+} (Singh et al., 2024), which pose significant health risks to humans and other living organisms due to their inability to naturally degrade in the environment (Li et al., 2019).

Manganese (Mn) is a naturally occurring element commonly found in surface and groundwater, with Mn^{2+} being its most stable form. Excess Mn^{2+} in drinking water can cause neurological disorders in humans, while high concentrations in aquatic environments can impair immunological functions in organisms such as fish (Ali, 2017; Wiśniowska-Kielian et al., 2015; Rudi et al., 2020). The World Health Organization (WHO) has established safe concentration limits for Mn in drinking water (0.05 mg/L) and natural water (0.1 mg/L) (Ali, 2017; Idrees et al., 2018).

Various methods are available for removing Mn^{2+} from wastewater, including filtration, coagulation, flocculation, and ion exchange. However, these methods are often costly and inefficient, particularly when heavy metal concentrations are high (Zamora-Ledezma et al., 2021). Adsorption is a recommended alternative due to its simplicity, cost-effectiveness, and safety for humans and animals (Li et al., 2019). The effectiveness of the adsorption process largely depends on the adsorbent's capacity, making the selection of an appropriate adsorbent critical. Cellulose is a promising organic adsorbent, offering advantages such as environmental friendliness, non-toxicity, cost efficiency, and functional groups capable of binding to metal ions (Lesbani et al., 2015).

Cellulose, a polysaccharide abundantly found in plant primary cell walls, is a water-insoluble biological macromolecule. Its adsorption capacity can be enhanced through surface modification using chemical methods like sulfation or oxidation of functional groups (Dachavaram et al., 2020). Sulfation transfers sulfonate groups (SO_3^-) to hydroxyl, amine, or carboxylic

acid groups (Alnouti, 2009). However, natural cellulose has limitations in heavy metal adsorption due to weak interactions between hydroxyl groups (-OH) and metal ions (Huang et al., 2019).

Oxidation of cellulose using 2,2,6,6-tetramethylpiperidine-1-oxyl (TEMPO) with NaOCl and NaBr converts primary hydroxyl groups (C6) into carboxylate groups (-COOH), resulting in negatively charged cellulose surfaces with improved adsorption capacity (Abou-Zeid et al., 2018). TEMPO acts as a catalyst in the oxidation process, influencing the reaction rate (Guan et al., 2019), while NaOCl serves as the primary oxidant to convert hydroxyl and residual aldehyde groups into carboxylates (Mishra et al., 2012).

This study focuses on modifying cellulose using TEMPO/NaOCl/NaBr to optimize Mn^{2+} adsorption by varying NaOCl concentrations (5, 15, and 30 mmol/g). The effect of NaOCl concentration on adsorption efficiency and cellulose properties was investigated through characterization techniques including scanning electron microscopy (SEM) to analyze surface morphology, X-ray diffraction (XRD) to determine crystal structure and purity, and Fourier Transform Infrared (FTIR) spectroscopy to identify functional groups in the modified cellulose.

Methods

Materials

Sodium hydroxide (NaOH, Glatt Chemical), sodium hypochlorite (NaOCl, Merck), 2,2,6,6-tetramethylpiperidine-1-oxyl (TEMPO), sodium bromide (NaBr, HiMedia Laboratories), distilled water, hydrochloric acid (HCl, BDA Chemical), sodium acetate (CH_3COONa, Merck), phenolphthalein indicator (Arkitos Chemical), and cellulose (Avicel PH 101), potassium permanganate ($KMNO_4$, KGsA), potassium periodate (KIO_4, Shanghai Z Chemical Co.,Ltd), manganese chloride tetrahydrate ($MnCl_2.4H_2O$, Xilong Scientific Co.,I.td), Phosphoric acid (H_3PO_4, Merck).

Cellulose oxidation with TEMPO/NaOCl/NaBr

A total of 0.08 g of 2,2,6,6-tetramethylpiperidin-1-oxyl (TEMPO) was dissolved in 750 mL of deionized water in a beaker under continuous stirring until completely dissolved. Subsequently, 10 g of cellulose was added to the TEMPO solution. Next, 0.5 g of NaBr and NaOCl (5 mmol/g) were added to the cellulose suspension. The pH of the solution was maintained between 10 and 11 by periodically adding 1 M NaOH. The suspension was stirred at room temperature for 2 hours to allow the oxidation reaction to proceed. After the reaction, the oxidized cellulose was thoroughly washed with distilled water to remove residual reagents and by-products. The TEMPO/NaOCl/NaBr oxidized cellulose was then dried at room temperature. The process was repeated using the same procedure with NaOCl concentrations of 15 mmol/g and 30 mmol/g to produce additional samples of oxidized cellulose under varying oxidation conditions.

Adsorption of Mn^{2+} with cellulose adsorbent

Adsorbent variations

Oxidized cellulose prepared with TEMPO/NaOCl/NaBr at concentrations of 5, 15, and 30 mmol/g was used as the adsorbent. For each variation, 0.1 g of the oxidized cellulose was weighed and added to a beaker containing 50 mL of Mn^{2+} solution. The mixture was stirred continuously for 60 minutes to allow adsorption to occur. Afterward, the mixture was filtered to separate the adsorbent from the filtrate. A 20 mL aliquot of the filtrate was transferred to a centrifuge tube, and 5 mL of 85% (w/w) H_3PO_4 and 0.4 g of KIO_4 were added. The solution was allowed to react until a purplish-pink color developed, indicating the presence of Mn^{2+}. The resulting samples were analyzed using a UV-Vis spectrophotometer to determine the residual Mn^{2+} concentration. The adsorption capacity with the highest efficiency from the initial test was used to further investigate the effects of different parameters, including adsorbent mass, contact time, and initial Mn^{2+} concentration, on the adsorption process.

Variation of adsorbent mass

TEMPO/NaOCl/NaBr oxidized cellulose was evaluated for its adsorption performance with Mn^{2+} solutions of 500 ppm concentration. Adsorbent masses of 0.01 g, 0.05 g, and 0.1 g were used. For each test, 50 mL of the Mn^{2+} solution was poured into a beaker, and the oxidized cellulose adsorbent was added to the solution. The mixture was stirred for 60 minutes to facilitate adsorption. After stirring, the solution was filtered to separate the adsorbent from the filtrate. The resulting filtrate was then treated according to the sub section adsorbent variations.

Variation of contact time

The oxidized cellulose adsorbent with the highest adsorption percentage from the initial mass variation study was selected for investigating the effect of contact time on Mn^{2+} adsorption. A 500 ppm Mn^{2+} solution (50 mL) was poured into separate beakers, and the selected cellulose adsorbent was added to each beaker. The adsorption process was conducted by stirring the mixtures using a magnetic stirrer for 30, 60, and 90 minutes. After the designated stirring times, the mixtures were filtered to separate the adsorbent from the filtrate. The resulting filtrate was then treated according to the sub section adsorbent variations.

Variation of Mn^{2+} concentration

The oxidized cellulose adsorbent with the highest adsorption efficiency from the mass and time variation studies was selected to evaluate the effect of Mn^{2+} solution concentration on adsorption performance. Mn^{2+} solutions with concentrations of 500, 1,000, and 1,500 ppm (100 mL each) were prepared in separate beakers, and the selected TEMPO/NaOCl/NaBr oxidized cellulose adsorbent was added to each beaker. The mixtures were stirred using a magnetic stirrer for the optimal adsorption time determined in the previous experiment. After stirring, the mixtures were filtered to

separate the cellulose adsorbent from the filtrate. The resulting filtrate was then treated according to the sub section *Adsorbent variations*.

Preparation and analysis of $KMnO_4$ standard solution

A total of 0.05 g of $KMnO_4$ was accurately weighed and dissolved in 50 mL of distilled water in a beaker to prepare a stock solution with a concentration of 1,000 ppm. The stock solution was then diluted to prepare standard solutions with concentrations of 10, 20, 30, 40, and 50 ppm. Each diluted solution was transferred into separate 15 mL centrifuge tubes. The standard solutions were analyzed using a UV-Vis spectrophotometer over a wavelength range of 200–700 nm. The absorbance data of the samples were recorded for further analysis.

Characterizations

Fourier transform infrared (FTIR)

The functional groups in TEMPO/NaOCl/NaBr oxidized cellulose were analyzed using a Cary 630 FTIR Agilent instrument. The cellulose samples were finely ground and mixed with KBr salt in a specific ratio. The mixture was subjected to high pressure to form thin, transparent KBr pellets. The prepared KBr pellets were carefully placed into a press holder to ensure uniform thickness and clarity. These pellets were then positioned in the FTIR instrument's sample compartment for analysis. FTIR measurements were conducted by recording the transmittance in the wavenumber range of 4000–500 cm^{-1} to identify the characteristic functional groups of the oxidized cellulose.

Scanning electron microscope (SEM)

The morphology of the TEMPO/NaOCl/NaBr oxidized cellulose adsorbent was analyzed using a scanning electron microscope (SEM). The sample was first coated with a thin layer of gold using a sputter coater to enhance conductivity and improve imaging quality. The gold-coated sample was then affixed onto a specimen holder using carbon tape to ensure stability during observation. The holder was inserted into the specimen chamber of the SEM device. The sample was examined at various magnifications to investigate its surface morphology and structural features, with images captured for further analysis.

X-ray diffraction (XRD)

X-ray diffraction (XRD) analysis was performed to determine the crystal structure, phase, and purity of cellulose and TEMPO/NaOCl/NaBr oxidized cellulose samples. The samples were prepared and analyzed using an XRD instrument to obtain diffraction patterns. The crystallinity of the samples was evaluated by comparing the interplanar spacing (d-spacing) and the intensity of the diffraction peaks with standard reference data. The presence of characteristic peaks was used to confirm the crystal structure and assess any changes in crystallinity due to the oxidation process. The diffraction patterns were analyzed to identify any new phases or alterations in the crystal structure, providing insights into the impact of the TEMPO/NaOCl/NaBr oxidation treatment on the cellulose samples. The crystallinity index was calculate according to the following equation:

$$\text{Crystallinity index} = \frac{Crystalline\ Intensity - Amorphous\ Intensity}{Crystalline\ Intensity}\ x\ 100\%$$

Results and Discussion

Synthesis of oxidized cellulose TEMPO/NaOCl/NaBr

The carboxyl group content in TEMPO/NaOCl/NaBr oxidized cellulose was quantified using the acid-base titration method. Oxidized cellulose samples prepared with NaOCl concentrations of 5, 15, and 30 mmol/g were titrated using 0.01 M HCl, 0.25 M sodium acetate, and 0.1 M NaOH, with phenolphthalein serving as the indicator. In this method, 0.01 M HCl was employed to acidify the cellulose surface, ensuring the protonation of carboxyl groups. Subsequently, 0.25 M sodium acetate was added as a buffering agent to stabilize the pH during titration. The titration process was performed using 0.1 M NaOH as the titrant, with the endpoint marked by a color change to pink, as illustrated in Fig-1. The data obtained from this titration procedure provided a precise determination of the carboxyl group content in the oxidized cellulose samples, highlighting the effect of varying NaOCl concentrations on the functionalization of cellulose.

Table 1. Carboxyl group content of TEMPO/NaOCl/NaBr oxidized cellulose

Variation (mmol/g)	Carboxyl group (mmol/g)
5	0.2393
15	0.2435
30	0.2664

The carboxyl group levels presented in Table 1 demonstrate that the addition of NaOCl as a primary oxidant effectively increases the carboxyl group content in the oxidized cellulose (Gamelas et al., 2015). The oxidation process utilizing TEMPO, combined with NaOCl, facilitates the conversion of aldehyde groups into carboxyl groups. Consequently, the carboxyl group levels become higher as the amount of NaOCl oxidant increases, reflecting the progression of oxidation (Lin et al., 2018).

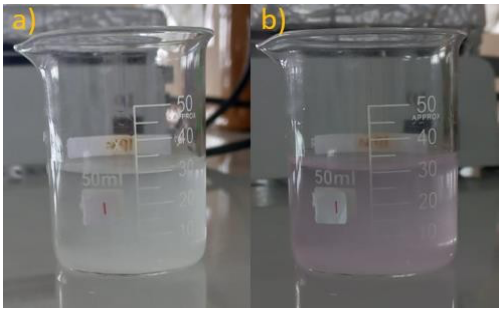

Fig-1. Results of acid-base titration, (a) before titration (b) after titration

Adsorption of Mn^{2+}

Variation of adsorbent

The Mn^{2+} adsorption test was conducted using TEMPO/NaOCl/NaBr oxidized cellulose adsorbents prepared with NaOCl concentrations of 5, 15, and 30 mmol/g to determine the optimum conditions for adsorption. The experiment utilized a Mn^{2+} solution with a concentration of 1,000 mg/L and a volume of 50 mL. The adsorption process was carried out for 60 minutes, after which the filtrate containing the unadsorbed Mn^{2+} was mixed with 85% H_3PO_4 and KIO_4. The addition of H_3PO_4 created an acidic environment essential for the color formation reaction, while KIO_4 served as an oxidizing agent to convert Mn^{2+} ions into MnO_4^- ions. This oxidation process was indicated by the solution changing color to purple. The resulting solution was analyzed using a UV-Vis spectrophotometer at a wavelength of 526 nm to determine the residual Mn^{2+} concentration. The linear regression equation obtained for the Mn^{2+} standard solution is y=0.1427x−0.0101, with a correlation coefficient (R^2) value of 0.9988. Table 2 presents the adsorption analysis results for TEMPO/NaOCl/NaBr oxidized cellulose with NaOCl concentrations of 5, 15, and 30 mmol/g.

Table 2. Percentage adsorption value for TEMPO/NaOCl/NaBr oxidized cellulose adsorbent types

Variation (mmol/g)	Average percentage adsorption (%)
5	92.40
15	91.71
30	91.43

The highest average adsorption percentage at the optimum conditions for TEMPO/NaOCl/NaBr oxidized cellulose was observed with the addition of 5 mmol/g NaOCl, achieving 92.40%. The addition of NaOCl as an oxidizer increases the carboxyl group content, thereby enhancing the negative surface charge and improving adsorption performance. However, as shown in Table 2, the adsorption percentage decreases with higher NaOCl concentrations. This reduction occurs because excessive NaOCl leads to the oxidation of secondary hydroxyl (OH) groups, resulting in the formation of undesired by-products, such as ketone groups, which disrupt the intended reaction pathway (Tartari et al., 2016; Abou-Zeid et al., 2018).

Variation of adsorbent mass

The oxidized cellulose with TEMPO/NaOCl/NaBr and a NaOCl concentration of 5 mmol/g demonstrated the highest adsorption percentage, making it the selected adsorbent for the variation in adsorbent mass experiments. Adsorbent mass is a critical factor influencing the adsorption process, as an increase in adsorbent mass generally provides a larger surface area for adsorption. In this study, the mass of TEMPO/NaOCl/NaBr oxidized cellulose (5 mmol/g NaOCl) was varied at 0.01 g, 0.05 g, and 0.1 g for adsorption of Mn^{2+} ions. The experiments were conducted using 50 mL of Mn^{2+} solution at a concentration of 500 mg/L with a contact time of 60 minutes. These mass variations were applied to evaluate the effectiveness of adsorbent quantity in the removal of Mn^{2+} ions. The percentage adsorption values obtained from the mass variation experiments are presented in Fig-2, providing insights into the relationship between adsorbent mass and adsorption efficiency.

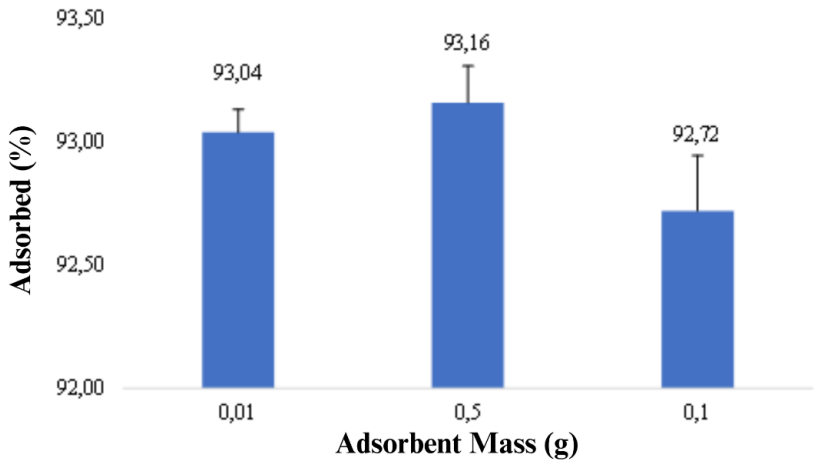

Fig-2. Effect of variation in adsorbent mass on the percentage adsorbed

The highest adsorption percentage for TEMPO/NaOCl/NaBr oxidized cellulose under optimum conditions was observed at a mass variation of 0.05 g, with an average adsorption percentage of 93.16%. As shown in Fig-2, the adsorption percentage decreased at a higher adsorbent mass of 0.1 g. While an increased adsorbent mass enhances the availability of active sites for Mn^{2+} adsorption, excessive mass can lead to a reduction in the adsorption rate due to saturation of the active sites. Additionally, increasing the adsorbent mass does not significantly improve the adsorption capacity, as most Mn^{2+} ions are adsorbed on the surface, reaching equilibrium conditions (Rudi et al., 2020). The optimum adsorbent mass of 0.05 g was subsequently used for the Mn^{2+} adsorption tests with varying contact times.

Variation of contact time

The optimum contact time for Mn^{2+} adsorption was determined using TEMPO/NaOCl/NaBr oxidized cellulose prepared with 5 mmol/g NaOCl. The adsorbent mass of 0.05 g, previously identified as optimal, was used in this study. Contact time variations of 30, 60, and 90 minutes were tested with a Mn^{2+} solution concentration of 500 mg/L. The percentage adsorption values obtained under these conditions are presented in Fig-3, highlighting the effect of contact time on adsorption efficiency and identifying the optimal duration for maximum adsorption.

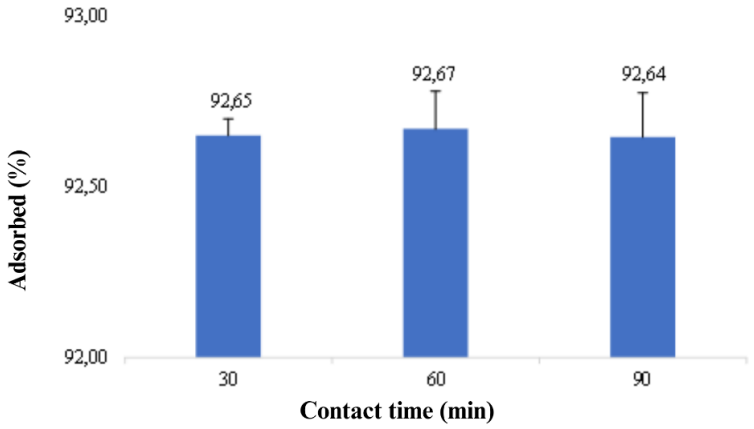

Fig-3. Effect of contact time variation on the percentage adsorption

The effect of contact time is a critical factor in the adsorption process, as it directly influences the adsorption efficiency of metal ions (Idrees et al., 2018). Contact time is defined by the reaction rate, which describes the change in concentration over time. As the contact time increases, more adsorbate molecules are absorbed onto the adsorbent surface until equilibrium is reached. For TEMPO/NaOCl/NaBr oxidized cellulose, the highest adsorption percentage under optimum conditions was achieved at a contact time of 60 minutes, with an average adsorption percentage of 92.67%. However, as shown in Fig-3, the adsorption percentage decreased at a contact time of 90 minutes. This reduction is attributed to partial saturation of the adsorbent surface, where the active sites can no longer adsorb additional Mn^{2+} ions due to the equilibrium state being reached (Akhyar et al., 2023). The optimum contact time of 60 minutes was subsequently used for Mn^{2+} adsorption tests at varying concentrations to evaluate the effect of initial Mn^{2+} concentration on adsorption efficiency.

Variation of Mn^{2+} concentration

The concentration of Mn^{2+} solution used to determine the optimum adsorption conditions was varied at 500, 1,000, and 1,500 mg/L. The mass of TEMPO/NaOCl/NaBr oxidized cellulose adsorbent (5 mmol/g NaOCl) was set at 0.05 g, and the contact time was fixed at 60 minutes based on the previously determined optimum conditions. The results obtained for the adsorption efficiency at different Mn^{2+} concentrations are presented in Fig- 4.

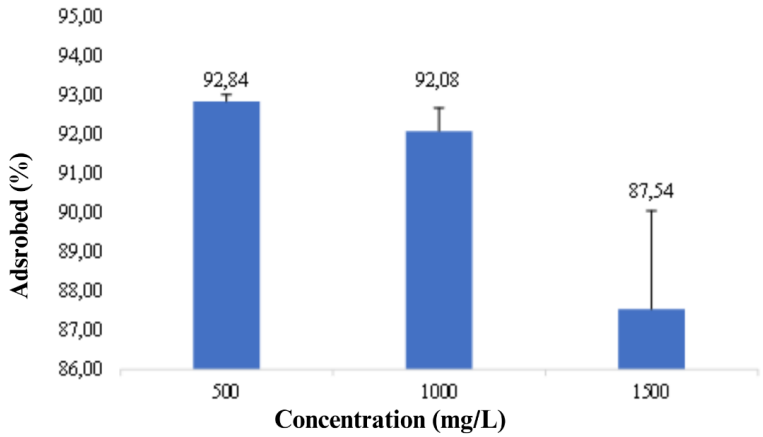

Fig-4 Effect of variations in Mn^{2+} solution concentration on the percentage adsorption

The optimum adsorption percentage was achieved at an Mn^{2+} solution concentration of 500 mg/L, with an average adsorption percentage of 92.84%. Generally, as the concentration of the adsorbate increases, the adsorption capacity of an adsorbent also increases and eventually reaches a maximum value at a certain concentration. However, in this study, as the Mn^{2+} solution concentration increased beyond 500 mg/L, the adsorption percentage decreased. This decline in adsorption percentage is attributed to the saturation of the active sites on the adsorbent surface, which reached equilibrium at higher Mn^{2+} concentrations. Since the mass of the TEMPO/NaOCl/NaBr oxidized cellulose adsorbent (5 mmol/g) remained constant, no additional active sites were available to accommodate the increased adsorbate concentration (Rudi et al., 2020).

Characterization

Fourier transform infrared (FTIR)

Pure cellulose and TEMPO/NaOCl/NaBr oxidized cellulose products with NaOCl concentrations of 5, 15, and 30 mmol/g were characterized using an FTIR instrument. The transmittance was measured across the wavenumber range of 4000–500 cm^{-1} to identify functional group changes resulting from the oxidation process. The FTIR characterization results are presented in Fig-5.

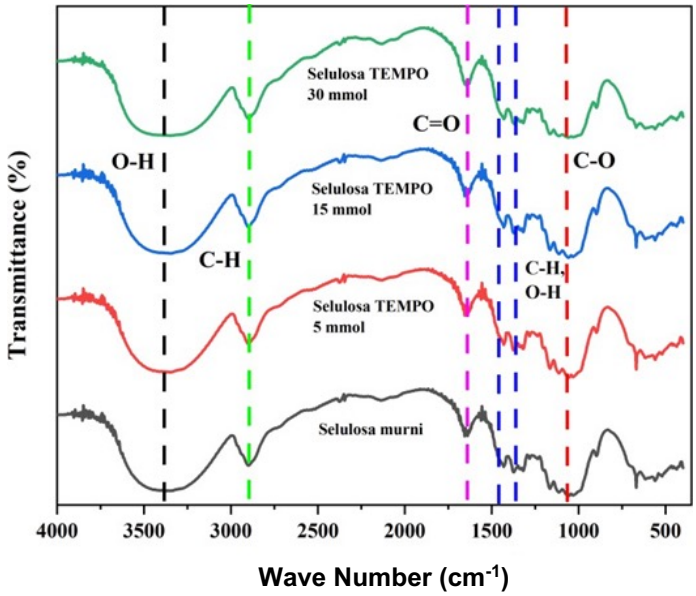

Fig-5. FTIR spectrum of pure cellulose and TEMPO/NaOCl/NaBr oxidized cellulose

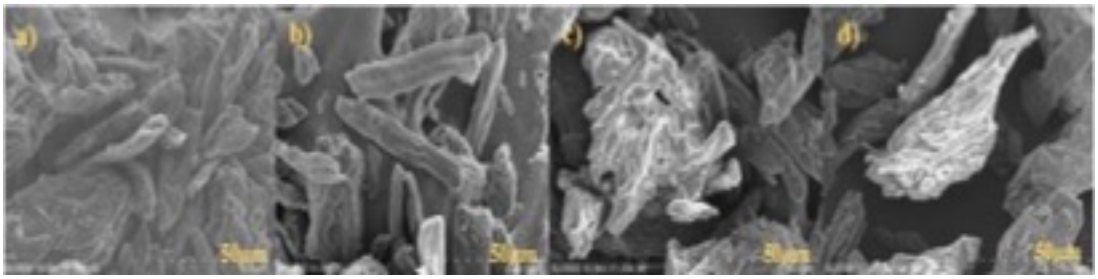

Fig-6. SEM morphology (a) pure cellulose (b) cellulose oxidized by 5 mmol/g NaOCl (c) cellulose oxidized by 15 mmol/g NaOCl (d) cellulose oxidized by 30 mmol/g NaOCl

The identification of absorption bands in the wavenumber range of 4000–500 cm^{-1} from Fig-5 provides insight into the structural differences between pure cellulose and TEMPO/NaOCl/NaBr oxidized cellulose with NaOCl concentrations of 5, 15, and 30 mmol/g. At 3358 cm^{-1}, a stretching vibration of the O-H group is observed, corresponding to the absorption band in the range of 3600–3000 cm^{-1}. This band represents the stretching vibration of O-H and strong intramolecular and intermolecular hydrogen bonds in cellulose, including those involving methyl and methylene groups (Pokhrel et al., 2020). The band at 2898 cm^{-1} is attributed to asymmetric and symmetric C-H stretching vibrations, corresponding to the absorption range of 2915–2820 cm^{-1}, which is characteristic of C-H stretches (Chen et al., 2020; Pokhrel et al., 2020). An absorption band at 1646 cm^{-1} is observed in oxidized cellulose, indicating the presence of C=O bonds. This shift results from the influence of counterions, specifically Na^+, confirming the successful oxidation of cellulose using TEMPO (Lomelí-Ramírez et al., 2018). The bands in the range of 1430–1381 cm^{-1} are associated with bending vibrations of C-H (CH_2) bonds, characteristic of type I cellulose. These also indicate the presence of O-H bending vibrations (Chen et al., 2020; Mondal et al., 2015). The band at 1063 cm^{-1} corresponds to the C-O group, originating from C-OH and C-O-C vibrations of the pyranose ring, which is a characteristic feature of cellulose. At 902–890 cm^{-1}, a band is observed that represents the typical structure of cellulose, specifically the β-1,4 glycosidic bonds connecting cellulose molecules (Pokhrel et al., 2020). These absorption

bands provide evidence of the structural modifications introduced during the TEMPO/NaOCl/NaBr oxidation process and confirm the retention of cellulose's characteristic features alongside the formation of oxidized functional groups.

Scanning electron microscope (SEM)

The surface morphology of pure cellulose and TEMPO/NaOCl/NaBr oxidized cellulose with NaOCl concentrations of 5, 15, and 30 mmol/g was analyzed to investigate the structural changes in the samples. This analysis provides insights into the surface features and modifications resulting from the oxidation process. The morphological analysis results are presented in Fig-6, highlighting the differences in surface structure between pure and oxidized cellulose. The morphological analysis of pure cellulose revealed the presence of irregular aggregates with highly varied particle sizes. In contrast, the morphology of TEMPO/NaOCl/NaBr oxidized cellulose at 5, 15, and 30 mmol/g NaOCl exhibited a more regular shape, attributed to the presence of anionic COONa groups densely distributed on the cellulose surface. Despite these modifications, the oxidized cellulose samples retained the core structural characteristics of pure cellulose (Isogai & Zhou, 2019). The width dimensions of pure cellulose and oxidized cellulose samples were measured using ImageJ software. The average width dimensions were found to be 0.068 µm for pure cellulose and 0.11 µm, 0.13 µm, and 0.43 µm for TEMPO/NaOCl/NaBr oxidized cellulose at 5, 15, and 30 mmol/g NaOCl, respectively.

X-ray diffraction (XRD)

XRD analysis was conducted on pure cellulose and TEMPO/NaOCl/NaBr oxidized cellulose samples with NaOCl concentrations of 5, 15, and 30 mmol/g to determine their crystal structure phases. The diffraction patterns obtained provide insights into the crystallinity and structural modifications resulting from the oxidation process. The results of the XRD analysis are presented in Fig-7.

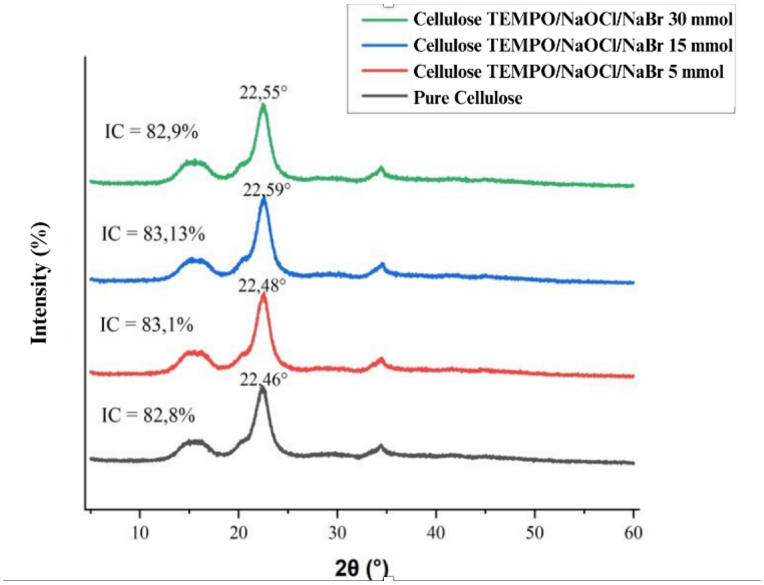

Fig-7 XRD analysis results

The XRD analysis results for pure cellulose and TEMPO/NaOCl/NaBr oxidized cellulose with NaOCl concentrations of 5, 15, and 30 mmol/g revealed diffraction peaks at 2θ values of 22.46°, 22.48°, 22.59°, and 22.55°, respectively. These peaks correspond to the characteristic crystalline structure of type I cellulose, which is identified by typical peaks at 2θ values of 14.8°, 16.4°, 22.6°, and 34.2° in pure cellulose (Mendoza et al., 2019). The diffraction patterns of oxidized cellulose show no significant changes compared to pure cellulose, indicating the oxidation resistance of type I cellulose crystals. This stability is attributed to the high crystallinity and low accessibility of the crystalline regions to reagents, preventing structural damage during the oxidation process (Tang et al., 2017). The crystallinity index, which provides information about the ratio of crystalline to amorphous structures in a sample, showed slight variations across the analyzed samples. The crystallinity index values were 82.8%, 83.1%, and 83.13% for pure cellulose, and TEMPO/NaOCl/NaBr oxidized cellulose with 5 and 15 mmol/g NaOCl, respectively. The increase in crystallinity is due to the selective oxidation reaction occurring predominantly in the amorphous regions of cellulose, which diminishes the amorphous content over time (Baron & Coseri, 2020). However, at a higher NaOCl concentration of 30 mmol/g, a decrease in crystallinity was observed. This reduction is likely due to the excessive addition of NaOCl, leading to increased oxidation in both amorphous and crystalline regions. The resulting increase in carboxyl groups and changes in the crystal structure contribute to the observed decrease in crystallinity (Nam et al., 2016).

Conclusion

The oxidation of cellulose using TEMPO/NaOCl/NaBr was successfully performed with NaOCl concentrations of 5, 15, and 30 mmol/g. The carboxyl group content increased with higher NaOCl concentrations, reaching 0.2393, 0.2435, and 0.2664 mmol/g, respectively. The adsorption efficiency of Mn^{2+} varied with the NaOCl concentration, achieving adsorption percentages of 92.40%, 91.71%, and 91.43%. The optimum adsorption condition was observed at 5 mmol/g NaOCl, with a

maximum adsorption percentage of 92.40%. FTIR analysis confirmed successful TEMPO oxidation, evidenced by a new absorption band at 1646 cm^{-1}, corresponding to the C=O bond in oxidized cellulose. XRD analysis showed an increase in the crystallinity index to 82.8%, 83.1%, and 83.13% for 5, 15, and 30 mmol/g NaOCl, respectively, indicating structural modifications due to oxidation.

Conflict of Interests

The author declares that there is no conflict of interest in this research and manuscript.

Acknowledgment

The authors would like to express their gratitude to Institut Teknologi Sumatera and the Laboratory of Materials and Environment, Department of Chemistry, for their invaluable support in conducting this study.

References

Abou-Zeid, R. E., Dacrory, S., Ali, K. A., & Kamel, S. (2018). Novel method of preparation of tricarboxylic cellulose nanofiber for efficient removal of heavy metal ions from aqueous solution. *International Journal of Biological Macromolecules*, 119, 207–214. https://doi.org/10.1016/j.ijbiomac.2018.07.127

Akhyar, Hesti Meilina, Fauzi Djuned, Sri Mulyati, & Abrar Muslim. (2023). Effectifity of dolomite adsorbent in purification of Mn and Cu from acid mine drainage. *International Journal of Social Science, Educational, Economics, Agriculture Research and Technology* (IJSET), 2(6), 86–96. https://doi.org/10.54443/ijset.v2i6.162

Ali, A. (2017). Removal of Mn(II) from water using chemically modified banana peels as efficient adsorbent. *Environmental Nanotechnology, Monitoring & Management*, 7, 57–63. https://doi.org/10.1016/j.enmm.2016.12.004

Alnouti, Y. (2009). Bile Acid Sulfation: A Pathway of Bile Acid Elimination and Detoxification. *Toxicological Sciences*, 108(2), 225–246. https://doi.org/10.1093/toxsci/kfn268

Baron, R. I., & Coseri, S. (2020). Preparation of water-soluble cellulose derivatives using TEMPO radical-mediated oxidation at extended reaction time. *Reactive and Functional Polymers*, 157, 104768. https://doi.org/10.1016/j.reactfunctpolym.2020.104768

Chen, Q., Xiong, J., Chen, G., & Tan, T. (2020). Preparation and characterization of highly transparent hydrophobic nanocellulose film using corn husks as main material. *International Journal of Biological Macromolecules*, 158, 781–789. https://doi.org/10.1016/j.ijbiomac.2020.04.250

Dachavaram, S. S., Moore, J. P., Bommagani, S., Penthala, N. R., Calahan, J. L., Delaney, S. P., Munson, E. J., Batta-Mpouma, J., Kim, J., Hestekin, J. A., & Crooks, P. A. (2020). A Facile Microwave Assisted TEMPO/NaOCl/Oxone (KHSO 5) Mediated Micron Cellulose Oxidation Procedure: Preparation of Two Nano TEMPO-Cellulose Forms. *Starch - Stärke*, 72(1–2). https://doi.org/10.1002/star.201900213

Gamelas, J. A. F., Pedrosa, J., Lourenço, A. F., Mutjé, P., González, I., Chinga-Carrasco, G., Singh, G., & Ferreira, P. J. T. (2015). On the morphology of cellulose nanofibrils obtained by TEMPO-mediated oxidation and mechanical treatment. *Micron*, 72, 28–33. https://doi.org/10.1016/j.micron.2015.02.003

Guan, Q., Chen, J., Chen, D., Chai, X., He, L., Peng, L., Zhang, J., & Li, J. (2019). A new sight on the catalytic oxidation kinetic behaviors of bamboo cellulose fibers under TEMPO-oxidized system: The fate of carboxyl groups in treated pulps. *Journal of Catalysis*, 370, 304–309. https://doi.org/10.1016/j.jcat.2019.01.003

Hasrini, R. F., Zakaria, F. R., Adawiyah, D. R., & Suparto, I. H. (2017). Mikroenkapsulasi Minyak Sawit Mentah dengan Penyalut Maltodekstrin dan Isolat Protein Kedelai. *Jurnal Teknologi Dan Industri Pangan*, 28(1), 10–19. https://doi.org/10.6066/jtip.2017.28.1.10

Huang, C.-F., Tu, C.-W., Lee, R.-H., Yang, C.-H., Hung, W.-C., & Andrew Lin, K.-Y. (2019). Study of various diameter and functionality of TEMPO-oxidized cellulose nanofibers on paraquat adsorptions. *Polymer Degradation and Stability*, 161, 206–212. https://doi.org/10.1016/j.polymdegradstab.2019.01.023

Idrees, M., Batool, S., Ullah, H., Hussain, Q., Al-Wabel, M. I., Ahmad, M., Hussain, A., Riaz, M., Ok, Y. S., & Kong, J. (2018). Adsorption and thermodynamic mechanisms of manganese removal from aqueous media by biowaste-derived biochars. *Journal of Molecular Liquids*, 266, 373–380. https://doi.org/10.1016/j.molliq.2018.06.049

Isogai, A., & Zhou, Y. (2019). Diverse nanocelluloses prepared from TEMPO-oxidized wood cellulose fibers: Nanonetworks, nanofibers, and nanocrystals. *Current Opinion in Solid State and Materials Science*, 23(2), 101–106. https://doi.org/10.1016/j.cossms.2019.01.001

Lesbani, A., Turnip, E. V., Mohadi, R., & Hidayati, N. (2015). Study Adsorption Desorption of Manganese(II) Using Impregnated Chitin-Cellulose as Adsorbent. *International Journal of Science and Engineering*, 8(2), 104–108. https://doi.org/10.12777/ijse.8.2.104-108

Li, M., Messele, S. A., Boluk, Y., & Gamal El-Din, M. (2019). Isolated cellulose nanofibers for Cu (II) and Zn (II) removal: performance and mechanisms. *Carbohydrate Polymers*, 221, 231–241. https://doi.org/10.1016/j.carbpol.2019.05.078

Lin, C., Zeng, T., Wang, Q., Huang, L., Ni, Y., Huang, F., Ma, X., & Cao, S. (2018). Effects of the Conditions of the TEMPO/NaBr/NaClO System on Carboxyl Groups, Degree of Polymerization, and Yield of the Oxidized Cellulose. *BioResource*, 3(13), 5965–5975.

Lomelí-Ramírez, M. G., Valdez-Fausto, E. M., Rentería-Urquiza, M., Jiménez-Amezcua, R. M., Anzaldo Hernández, J., Torres-Rendon, J. G., & García Enriquez, S. (2018). Study of green nanocomposites based on corn starch and cellulose nanofibrils from Agave tequilana Weber. *Carbohydrate Polymers*, 201, 9–19. https://doi.org/10.1016/j.carbpol.2018.08.045

Mendoza, D. J., Browne, C., Raghuwanshi, V. S., Simon, G. P., & Garnier, G. (2019). One-shot TEMPO-periodate oxidation of native cellulose. *Carbohydrate Polymers*, 226, 115292. https://doi.org/10.1016/j.carbpol.2019.115292

Mishra, S. P., Manent, A.-S., Chabot, B., & Daneault, C. (2012). The Use of Sodium Chlorite in Post-Oxidation of TEMPO-Oxidized Pulp: Effect on Pulp Characteristics and Nanocellulose Yield. *Journal of Wood Chemistry and Technology*, 32(2), 137–148. https://doi.org/10.1080/02773813.2011.624666

Mondal, Md. I. H., Yeasmin, Mst. S., & Rahman, Md. S. (2015). Preparation of food grade carboxymethyl cellulose from corn husk agrowaste. *International Journal of Biological Macromolecules*, 79, 144–150. https://doi.org/10.1016/j.ijbiomac.2015.04.061

Nam, S., French, A. D., Condon, B. D., & Concha, M. (2016). Segal crystallinity index revisited by the simulation of X-ray diffraction patterns of cotton cellulose Iβ and cellulose II. *Carbohydrate Polymers*, 135, 1–9. https://doi.org/10.1016/j.carbpol.2015.08.035

Pokhrel, S., Shrestha, M., Slouf, M., Sirc, J., & Adhikari, R. (2020). Eco-Friendly Urea-Formaldehyde Composites Based on Corn Husk Cellulose Fiber. *International Journal of Composite Materials*, 2020(2), 29–36. https://doi.org/10.5923/j.cmaterials.20201002.01

Rudi, N. N., Muhamad, M. S., Te Chuan, L., Alipal, J., Omar, S., Hamidon, N., Abdul Hamid, N. H., Mohamed Sunar, N., Ali, R., & Harun, H. (2020). Evolution of adsorption process for manganese removal in water via agricultural waste adsorbents. *Heliyon*, 6(9), e05049. https://doi.org/10.1016/j.heliyon.2020.e05049

Sawka, M. N., Cheuvront, S. N., & Carter, R. (2005). Human Water Needs. *Nutrition Reviews*, 63, S30–S39. https://doi.org/10.1111/j.1753-4887.2005.tb00152.x

Singh, V., Ahmed, G., Vedika, S., Kumar, P., Chaturvedi, S. K., Rai, S. N., Vamanu, E., & Kumar, A. (2024). Toxic heavy metal ions contamination in water and their sustainable reduction by eco-friendly methods: isotherms, thermodynamics and kinetics study. *Scientific Reports*, 14(1). https://doi.org/10.1038/s41598-024-58061-3

Tang, Z., Li, W., Lin, X., Xiao, H., Miao, Q., Huang, L., Chen, L., & Wu, H. (2017). TEMPO-Oxidized Cellulose with High Degree of Oxidation. *Polymers*, 9(9), 421. https://doi.org/10.3390/polym9090421

Tartari, T., Bachmann, L., Maliza, A. G. A., Andrade, F. B., Duarte, M. A. H., & Bramante, C. M. (2016). Tissue dissolution and modifications in dentin composition by different sodium hypochlorite concentrations. *Journal of Applied Oral Science*, 24(3), 291–298. https://doi.org/10.1590/1678-775720150524

Wiśniowska-Kielian, B., Wiśniowska-Kielian, B., & Niemiec, M. (2015). Accumulation of manganese in selected links of food chains in aquatic ecosystems. *Journal of Elementology*, 4/2015. https://doi.org/10.5601/jelem.2015.20.1.808

Zamora-Ledezma, C., Negrete-Bolagay, D., Figueroa, F., Zamora-Ledezma, E., Ni, M., Alexis, F., & Guerrero, V. H. (2021). Heavy metal water pollution: A fresh look about hazards, novel and conventional remediation methods. *Environmental Technology & Innovation*, 22, 101504. https://doi.org/10.1016/j.eti.2021.101504